Optics Communications 336 (2015) 319–325

Contents lists available at ScienceDirect

Optics Communications

journal homepage: www.elsevier.com/locate/optcom

Direct fluorescence characterisation of a picosecond seeded optical parametric amplifier

N.H. Stuart *, D. Bigourd [1], R.W. Hill, T.S. Robinson, K. Mecseki, S. Patankar, G.H.C. New, R.A. Smith

Blackett Laboratory, Imperial College London, Prince Consort Road, South Kensington, London SW7 2AZ, UK

ARTICLE INFO

Article history:
Received 21 July 2014
Received in revised form
8 September 2014
Accepted 10 September 2014
Available online 29 September 2014

Keywords:
Optical parametric amplification
Parametric fluorescence
Pulse temporal contrast

ABSTRACT

The temporal intensity contrast of high-power lasers based on optical parametric amplification (OPA) can be limited by parametric fluorescence from the non-linear gain stages. Here we present a spectroscopic method for direct measurement of unwanted parametric fluorescence widely applicable from unseeded to fully seeded and saturated OPA operation. Our technique employs simultaneous spectroscopy of fluorescence photons slightly outside the seed bandwidth and strongly attenuated light at the seed central wavelength. To demonstrate its applicability we have characterised the performance of a two-stage picosecond OPA pre-amplifier with 2.8×10^5 gain, delivering 335 μJ pulses at 1054 nm. We show that fluorescence from a strongly seeded OPA is reduced by $\sim500\times$ from the undepleted to full pump depletion regimes. We also determine the vacuum fluctuation driven noise term seeding this OPA fluorescence to be 0.7 ± 0.4 photons ps^{-1} nm^{-1} bandwidth. The resulting shot-to-shot statistics highlights a 1.5% probability of a five-fold and 0.3% probability of a ten-fold increase of fluorescence above the average value. Finally, we show that OPA fluorescence can be limited to a few-ps pedestal with 3×10^{-9} temporal intensity contrast 1.3 ps ahead of an intense laser pulse, a level highly attractive for large scale chirped-pulse OPA laser systems.

1. Introduction

Optical parametric chirped pulse amplification (OPCPA) is a rapidly developing area of ultrashort laser technology with the potential to simultaneously increase the pulse energy and bandwidth in addition to the enhancement of the temporal intensity contrast (the ratio of optical noise or pre-pulse to the primary laser pulse peak intensity) when compared to gain-storage chirped-pulse amplification systems [1]. For high peak-power experiments, using focussed laser intensities of $>10^{19}$ W/cm^2, a temporal intensity contrast of $>10^8$ is highly desirable to avoid unwanted perturbation of a fragile target or pre-plasma formation before the arrival of the main pulse. For laser systems adopting the OPCPA architecture, spontaneous parametric fluorescence of phase-matched signal and idler pairs in the presence of a strong pump pulse in the optical parametric amplifiers (OPA) is an important source of incoherent noise. The generation and further amplification of fluorescence can be modelled semi-classically as zero-point fluctuations of the electromagnetic field [2] contributing an initial seed term to the OPA process that is then amplified in parallel with the main laser seed. This fluorescence typically forms a pedestal of similar duration to the OPA pump pulse around the primary pulse and is frequently reported to be the main contrast limitation in many OPCPA systems [3–6].

Previous research has reported on methods to reduce the contrast degrading effects of parametric fluorescence, such as limiting the gain per non-linear amplifier [7] or the use of OPCPA pre-amplification with shorter seed and pump durations to confine the fluorescence within a smaller time window [8]. The temporal contrast characterisation of high peak-power lasers is typically performed using a third-order autocorrelator [9], which are able to provide high dynamic range ($>10^{10}$) measurements that can distinguish between optical noise ahead of or behind the primary pulse. However, observation of parametric fluorescence with a third-order autocorrelation will contain many other sources of noise (e.g. from grating scatter or incomplete recompression due to high-order phase effects), as the diagnostic needs to be placed after the short-pulse compressor to properly resolve the fluorescence. Additional amplifier stages may also be required to generate sufficient intensity for efficient operation of the non-linear processes used in an autocorrelator, which will contribute their own noise terms. As a result, empirical measurements of the behaviour of parametric fluorescence from unseeded to fully seeded OPA operation have not been reported to date in the literature.

* Corresponding author.
E-mail address: nicholas.stuart@imperial.ac.uk (N.H. Stuart).
[1] Current Address: CNRS-Université Lille 1, PhLAM/IRCICA USR 3380/UMR 8523, F-59655 Villeneuve d'Ascq Cedex, France.

http://dx.doi.org/10.1016/j.optcom.2014.09.032

Measuring the unseeded fluorescence is a common method of characterisation that assumes that less fluorescence will be generated when in competition with the amplification of the primary laser seed. [5,10,11]. Dorrer et al. presented a high-contrast OPCPA pre-amplifier system, generating energies of $\sim 100\,\mu J$ with $< 20\,\mu J$ of fluorescence in an unseeded mode of operation, where the primary laser seed is blocked and the non-linear crystals were still optically pumped [5]. A fluorescence contrast of $\sim 10^4$ was observed in the fully seeded mode using a third-order autocorrelator. However, the physical mechanisms responsible for the discrepancy in the fluorescence intensity between these two modes of operation were not explored.

We present a simple technique to determine the parametric fluorescence contrast produced from a seeded OPA process by measuring the spectral intensity of fluorescence that lies slightly outside the full bandwidth of the seed. We demonstrate its ability to measure and distinguish the parametric fluorescence intensity simultaneously with the OPA signal for the full range of unseeded to strongly seeded operation. The experimental determination of the noise term found in the OPAs and its mechanism of amplification will be of benefit to modelling OPCPA system performance and in assessing the potential impact of parametric pre-pulse in high-intensity laser–matter interaction experiments.

2. Experiment setup

2.1. OPCPA laser

The OPCPA system used to demonstrate the measurement and characterisation of parametric fluorescence in a seeded OPA process (Fig. 1) is similar to the designs reported by Dorrer et al. [5] and Musgrave et al. [8]. A master oscillator producing 3 nJ, 250 fs transform-limited pulses centred at 1054 nm provides both the short-pulse seed and a source for the generation of optically locked pump pulses of up to 2.2 mJ, 6 ps for two picosecond-regime OPAs (termed ps-OPA here for clarity) operating near degeneracy using beta barium borate (BBO) as the non-linear media. A non-collinear angle of 0.6° between the seed and the pump allows spatial separation of the signal, idler and pump pulses after amplification. These ps-OPA stages produce 335 μJ of amplified signal from a 1.2 nJ seed that is pre-stretched to 1.25 ps with four-passes of a 30 cm H-ZF7LA glass block. Optimal energy, bandwidth and stability are achieved when each stage saturates the available pump energy at the temporal intensity centre. Beyond this point, further amplification will result in back-conversion of energy from the signal to the pump, which is monitored with a spectrometer.

The amplified signal is then stretched again to 1.6 ns in a reflective Öffner grating system and used to seed a pair of nanosecond-regime OPAs (ns-OPA) to produce a 20 mJ seed for an Nd:Glass power amplifier chain. The details of the ps-OPA design and operation have previously been reported [12]. The main system parameters of the ps-OPAs we investigate here are presented in Table 1.

The amplifiers have been designed to reduce contrast degradation from parametric fluorescence by ensuring the seed pulse overfills the spatial profile of the pump, while the temporal profile is optimised to provide a balance between bandwidth enhancement and energy extraction from the pump [12]. Each stage is single-passed to avoid pre-pulse generation from stray reflections, with spatial filtering between the stages to eliminate wide-angle propagation of parametric fluorescence.

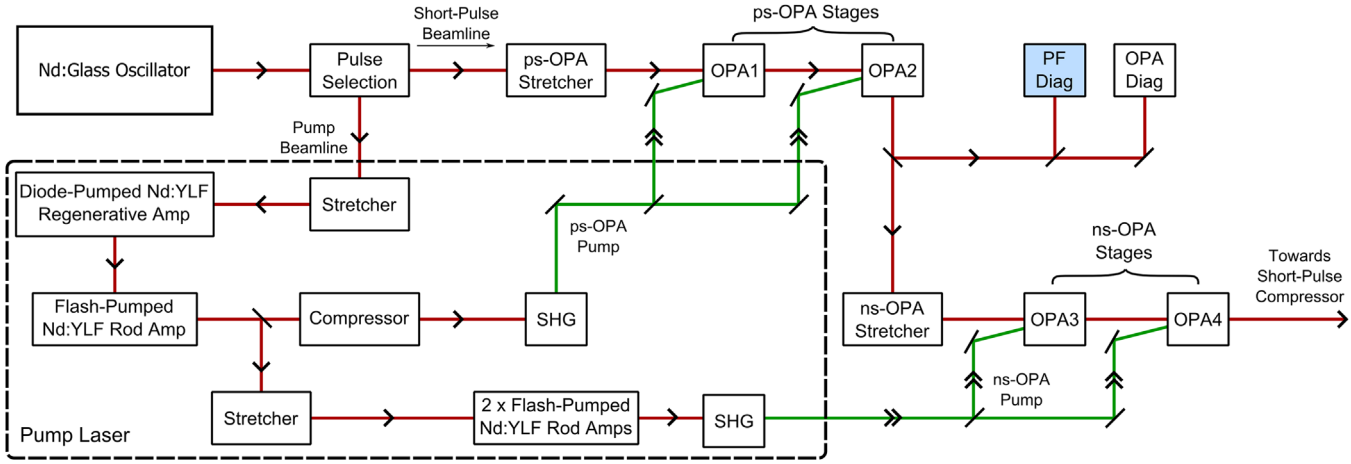

Fig. 1. Simplified setup of the OPCPA laser frontend. 'PF Diag' indicates where the unseeded and seeded parametric fluorescence were measured unless otherwise stated.

Table 1
Key operating parameters of the ps-OPA stages used for the parametric fluorescence characterisation. Pulse bandwidth, duration and diameter are quoted as full-width at half-maximum unless otherwise stated.

Crystal	**OPA Stage 1 (OPA1)** 6.5 mm BBO (Type I)			**OPA Stage 2 (OPA2)** 2 mm BBO (Type I)		
	Seed	*Pump*	*Signal*	*Seed*	*Pump*	*Signal*
Wavelength	1054.5 nm	526.5 nm	1054 nm	1054 nm	526.5 nm	1054 nm
Bandwidth	4 nm	0.5 nm	5.9 nm	5.9 nm	0.5 nm	8.7 nm
Energy	1.2 nJ	230 μJ	20 μJ	20 μJ	1.82 mJ	335 μJ
Duration	1.25 ps	6 ps	~1.8 ps	~1.8 ps	6 ps	2.6 ps
Diameter	820 μm	870 μm	850 μm	1.8 mm	1.1 mm	1.3 mm
Diameter ($1/e^2$)	1.7 mm	1.7 mm	1.65 mm	2.7 mm	2.2 mm	1.8 mm
Peak Intensity	130 kW/cm^2	4.2 GW/cm^2	1.3 GW/cm^2	0.3 GW/cm^2	200 GW/cm^2	6.3 GW/cm^2

When both ps-OPAs were pumped with the primary laser seed blocked, approximately 1 nJ of parametric fluorescence was observed after the Öffner stretcher before injection into the ns-OPAs. The Öffner stretcher has a finite spectral acceptance of 1054 ± 10 nm with 35% energy transmission efficiency and delivers ~ 110 μJ of primary laser seed for the subsequent amplifiers.

A cross-correlation of the parametric fluorescence from OPA1 seeding a pumped OPA2 (Fig. 2) yields a ~ 2.1 ps pulse duration of the parametric fluorescence generated in the ps-OPAs, which agrees well with Dorrer et al.. [5], who use similar ps-OPA parameters.

After the short-pulse compressor, using a pair of 1740 lines/mm gratings matched to the combination of the bulk material and grating stretchers, the incoherent parametric fluorescence is expected to have a negligible residual chirp of -0.152 ps^2, as it does not pass through the bulk material stretcher. The transform-limit of the OPA2 output is ~ 185 fs but gain narrowing from temporal windowing in the ns-OPAs and spectral narrowing in the subsequent Nd:Glass gain-storage amplifiers produce a final compressed pulse duration of 500 fs for multi-terawatt interactions with targets.

Using only this unseeded parametric fluorescence noise term from the ps-OPAs, a $1{:}10^5$ energy ratio and a $\sim 4{:}1$ pulse duration ratio are expected between the fluorescence and the primary laser pulse after compression. Therefore, in the worst case that parametric fluorescence remains unchanged in the strongly seeded mode of operation, the temporal intensity contrast ratio of the parametric fluorescence contribution from the ps-OPAs to the amplified and compressed primary pulse, as illustrated in Fig. 3, is expected to be $\sim 6 \times 10^{-6}$ at 1.1 ps before the peak of the primary pulse.

Before this time, the fluorescence will be stronger than the temporal wings of the amplified short-pulse and will therefore be a limiting term in applications such as ultrafast, high-intensity laser–matter interaction experiments.

2.2. Seeded OPA fluorescence diagnostic

The fluorescence produced from an OPA reflects the phase-matched wavelengths and emission directions relative to the strong pump pulse. A broad phase-matched bandwidth is possible in the case of degenerate interactions using a few millimetres of a highly non-linear material such as BBO with a small angle between the pump and the seed to separate the OPA signal and the idler. In our setup, this has been measured, as shown in Fig. 4, by focussing the combined fluorescence from OPA1 and OPA2 that is emitted in the same direction as the seed into a spectrometer

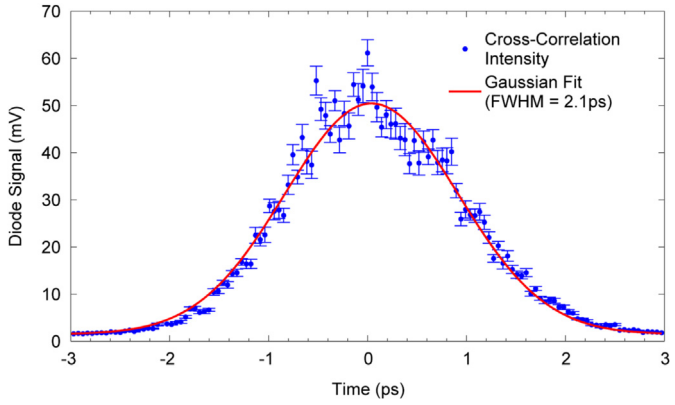

Fig. 2. Cross-correlation between the OPA2 pump and parametric fluorescence generated in OPA1. A 2.1 ps pulse is retrieved after a $\sqrt{2}$ deconvolution factor for Gaussian pulses is applied.

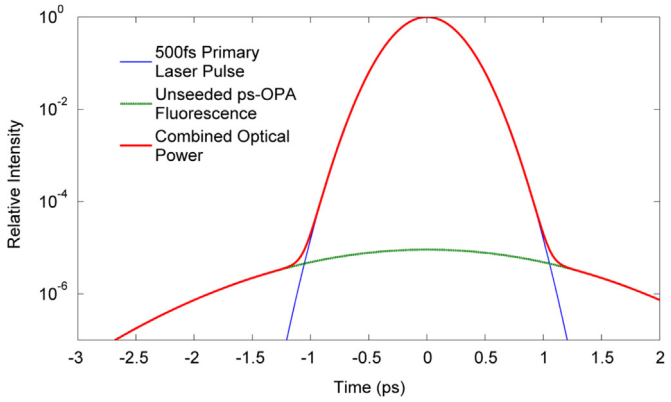

Fig. 3. Expected unseeded ps-OPA parametric fluorescence of 2.1 ps duration temporal intensity contrast versus the 500 fs primary laser pulse after the final compressor. Gaussian pulse shapes are assumed for the primary laser pulse and unseeded ps-OPA fluorescence.

(OceanOptics USB4000) approximately 1 m downstream from OPA2. It should be noted that the fluorescence from OPA1 could not be detected on its own and the removal of the spatial filter between the OPA stages had no noticeable effect on the shape of the fluorescence spectrum. Furthermore, tightening of the spatial filter aperture size also had no effect on the fluorescence observed, indicating that the fluorescence photons observed are collimated and follow the same path as the primary laser seed. The phase-matched bandwidth covers ~ 200 nm centred at 1020 nm in the emission direction of the seed, which is slightly offset relative to the 1054 nm main laser seed due to the 0.6° non-collinear angle between the pump and seed pulses [13].

The spectral offset between fluorescence and laser seed for non-collinear OPA helps to reduce contrast degradation, as any fluorescence produced outside of the final compressor spectral acceptance window will be filtered out very efficiently. The ns-OPA stretcher and the final compressor used here both have a finite bandwidth acceptance of 20 nm from 1044 nm to 1064 nm. Thus, only 12% of the broadband fluorescence energy from the ps-OPAs will propagate through the system.

The broad fluorescence spectrum produced relative to the narrowband OPA seed provides the opportunity to spectrally distinguish the fluorescence emission simultaneously with amplification of a strong seed without saturating or damaging the spectrometer.

In our case, an ideal transform-limited 250 fs Gaussian mode-locked laser seed pulse centred at 1054 nm will have a relative spectral intensity of $< 10^{-90}$ at wavelengths less than 1 μm i.e. there are essentially zero laser seed photons at these wavelengths where the fluorescence emission is strong.

For this implementation, high-reflectivity 0° incidence Nd:YAG laser-line dielectric mirrors (CVI Laser Optics) acted as a spectral band-stop filter between 980 nm and 1170 nm, with a high damage threshold able to withstand the fully amplified OPA signal. As these mirrors are also used to transport the pulses in the laser beamline, the OPA seed will be significantly attenuated outside of this bandwidth acceptance e.g. residual CW/spontaneous emission from the mode-locked oscillator. This provides further discrimination between seed and fluorescence wavelengths. The amount of attenuation expected from a single filter is of the order 10^3 and therefore multiple filters were stacked in series to sufficiently attenuate the $> 10^5$ more intense fully amplified primary OPA signal compared to the fluorescence. This optical setup (Fig. 5a) was positioned approximately 1 m after the second ps-OPA stage without any mirrors in between to capture the full bandwidth emission of the amplifiers.

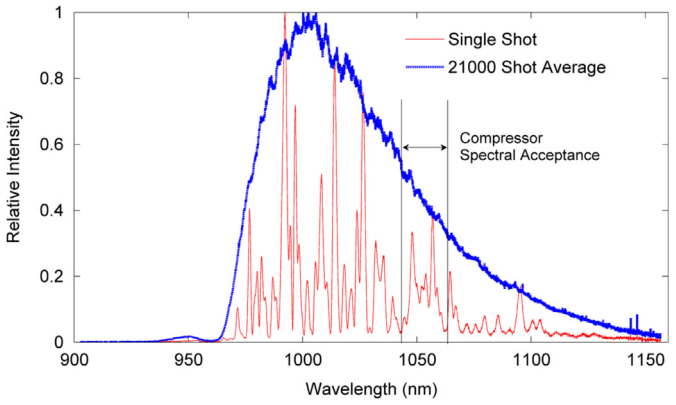

Fig. 4. Unseeded parametric fluorescence spectrum emitted in the seed direction of the ps-OPAs with a 0.6° non-collinear angle. (Red solid line) Instantaneous fluorescence from a single shot, illustrating the random probabilistic nature of parametric down-conversion and subsequent amplification. (Blue dotted line) Averaged parametric fluorescence over 21,000 shots, highlighting the broad phase-matching achieved and the peak wavelength offset of parametric fluorescence in non-collinear geometries. In this case the seed is centred at 1054 nm and the fluorescence at 1020 nm, which acts to improve contrast for narrowband OPCPA schemes. The spectral non-linearity of the detector has been calibrated to a known 3100 K blackbody source. (For interpretation of the references to colour in this figure caption, the reader is referred to the web version of this paper.)

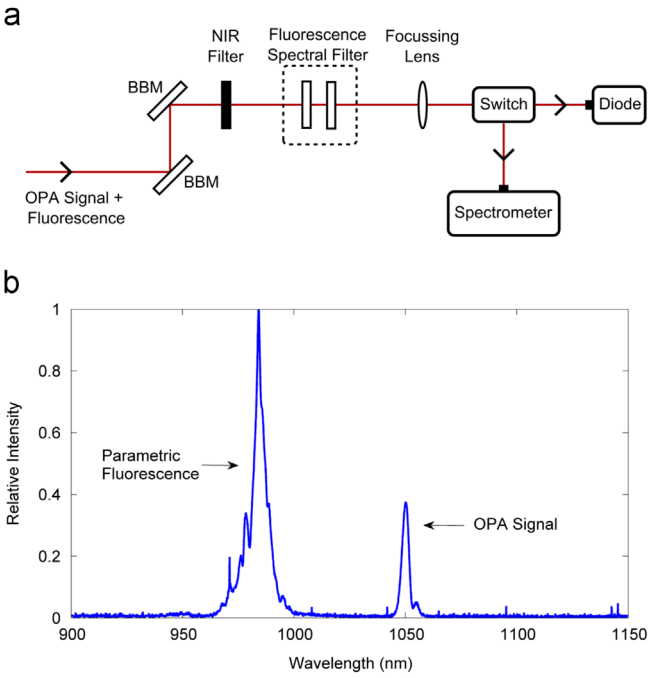

Fig. 5. (a) Optical layout of the parametric fluorescence diagnostic. Broadband mirrors (BBM) are used to transport and avoid spectral distortion of the OPA output. The main amplified signal is spectrally attenuated using stacked short-pass filtering. The effectiveness of the filter stack was determined using a well calibrated spectrometer before the energy characterisation using a photodiode. A long-pass filter was used to block any residual shorter wavelength pump light or weak SHG generation from the OPA. (b) Experimental data showing the effectiveness of spectral filtering using two stacked filters to simultaneously resolve the fluorescence and primary amplified OPA signal spectrum. Additional filters were inserted to fully extinguish the OPA signal to characterise the fluorescence from the seeded OPAs.

The photodiode used for retrieval of the absolute fluorescence energy was first calibrated with a power meter against the 70 MHz seed oscillator pulses without any filtering. The attenuation factor from the spectral filter stack was then determined using the unseeded fluorescence photodiode signal to give a final system calibration. The spectral non-linearity of the photodiode was also factored into the data analysis.

A key assumption of this characterisation is that changes in the parametric fluorescence spectral intensity slightly outside of the seed bandwidth also reflect the behaviour of wavelengths overlapped within the OPA seed/signal that cannot be directly measured. As noise photons are uncorrelated and the phase-matching conditions of the amplifier should not change between unseeded and seeded operation i.e. the shape of the fluorescence spectrum in Fig. 4 should not change, we believe this to be a robust hypothesis.

A critical requirement for this characterisation method is that the parametric fluorescence bandwidth exceeds the bandwidth of the main OPA laser seed to allow the use of an edge-pass filter stack to attenuate the significantly stronger seeded OPA signal. While this is aided by using a non-collinear geometry to offset the peak emission wavelength of fluorescence observed, this method will most likely become more difficult to implement for ultra-broadband OPCPA systems designed for few-cycle amplification. In such a scheme, the parametric fluorescence may need to be observed at a different viewing angle to the seed/signal with optical scatter minimised to allow the weak fluorescence emission to be resolved.

We acknowledge the work of Tavella et al. [10], who reported a conceptually similar technique using a dazzler to produce a spectral hole in the OPA seed and measured the fluorescence generation at a comparable intensity to the OPA signal. However, for high dynamic range contrast characterisation, such a device will need to completely attenuate the seed bandwidth to levels less than the few tens of photons of the fluorescence seed, which is unrealistic for any active electro-optic device. The spectral-hole technique is not able to strongly attenuate the fluorescence relative to the signal, therefore only low dynamic-range measurements ($\sim 10^2$) are possible. Measuring the fluorescence outside of the seed bandwidth, as we demonstrate here, allows far higher-dynamic range characterisation without the requirement to add an extra optical setup to completely remove part of the seed bandwidth e.g. a dispersive system with a Fourier-plane mask.

3. Seeded ps-OPA fluorescence results and analysis

With a diagnostic able to measure the fluorescence emission from a seeded OPA operating at full power, it is possible to examine the parametric fluorescence behaviour when in direct competition with amplification of the primary laser seed.

A common method to rapidly diagnose the potential impact of fluorescence on the compressed temporal contrast is to measure the unseeded OPA output and its behaviour as a function of the pump energy. Fig. 6 shows the unseeded and fully seeded parametric fluorescence energy plotted as a function of pump energy. In both cases the fluorescence generated from the ps-OPAs rises exponentially with increasing pump energy, though with different coefficients, which is expected for small signal gain as a function of pump energy. When the ps-OPA stages are operating in saturation with 2.05 mJ total pump energy, the unseeded and seeded fluorescence energies are 8.2 nJ and 100 pJ respectively.

The characterisation of the fluorescence generated in these ps-OPAs represents a significant step towards understanding its impact on temporal contrast. With such a device, the fluorescence emission from the OPAs can be quantified to a higher dynamic range than with an autocorrelator, as the dynamic range is directly related to the number of spectral filters added. The fast acquisition from the photodiode detector enables optimisation of the parameters of the laser that affect the parametric fluorescence intensity.

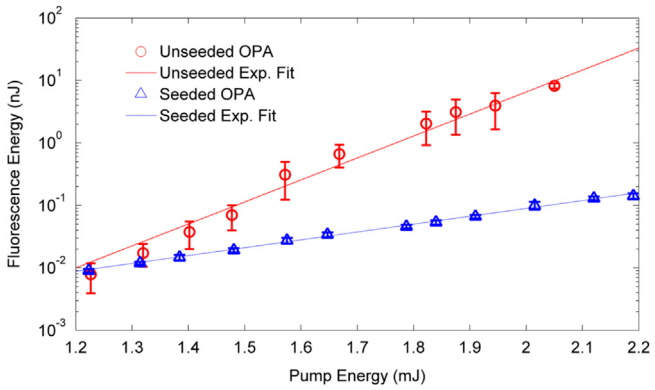

Fig. 6. Parametric fluorescence energy generated from the ps-OPAs as a function of the total pump energy for the unseeded amplifier (red circles) and the fully seeded case (blue triangles). (For interpretation of the references to colour in this figure caption, the reader is referred to the web version of this paper.)

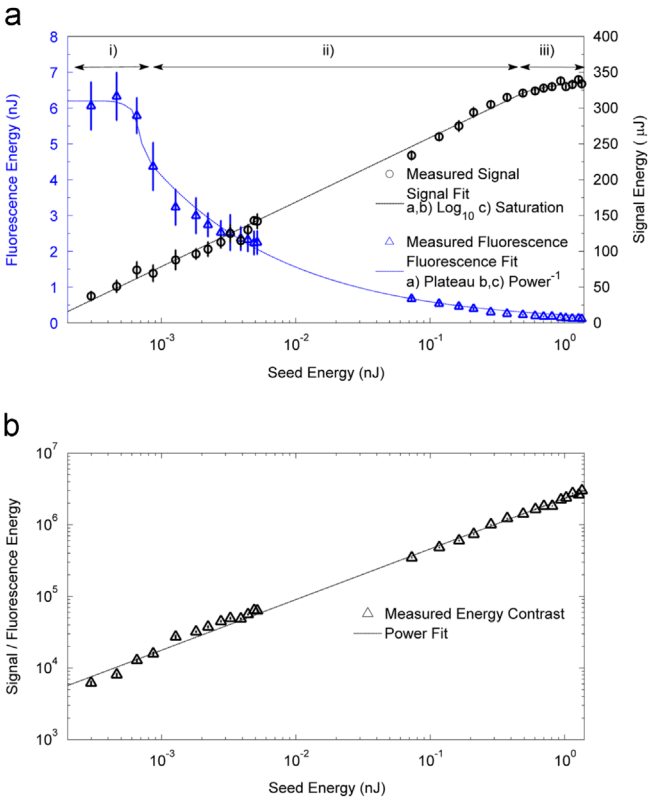

Fig. 7. (a) Measured parametric fluorescence (blue triangles) in competition with the OPA seed (black circles). Three regimes of amplification behaviour are identified, from (i) the undepleted pump regime, where fluorescence is broadly similar to the unseeded case, (ii) the onset of pump depletion, where the fluorescence intensity becomes strongly quenched with less available pump, and (iii) strong pump depletion, where the pump intensity centre becomes comparable to them main laser signal, creating a gain saturation effect. (b) Energy contrast between the ps-OPA signal and fluorescence as a function of the seed energy. Fluorescence contrast enhancement from the finite spectral acceptance window of the compressor has been excluded. (For interpretation of the references to colour in this figure caption, the reader is referred to the web version of this paper.)

From Fig. 6, the fluorescence is clearly seen to be in competition with the amplification of the primary laser seed. Evidence for the physical mechanism behind this behaviour is best illustrated in Fig. 7a, which investigates the total fluorescence from both stages as a function of the seed energy into the first ps-OPA stage.

At low seed levels, the OPA operates in the undepleted pump regime for seed energies <0.7 pJ (case i). As the residual pump temporal profile is difficult to retrieve, the amount of pump depletion was cross-checked against a 1D OPA code previously used to design the ps-OPA stages [12], which predicts $>0.5\%$ pump depletion at the temporal intensity maxima for seed energies >1 pJ. The level of pump depletion increases with greater seed energies (case ii) until the amplified signal reaches the maximum saturation point of 335 μJ, i.e. before energy back-conversion at the temporal intensity centre (case iii). A key point is that the fluorescence in the undepleted pump regime for a seeded OPA agrees with the fluorescence generated for the unseeded case with equal pump energy and therefore it is reasonable to expect that seed energies less than the range measured are not likely to change the fluorescence emission characteristics.

For larger seed energies, the greater pump depletion leads to weaker fluorescence emission, following an inverse power relationship. In the saturation regime (case iii), there is little change in net available pump energy and therefore the observed fluorescence remains approximately constant. At the saturation point, the combined ps-OPA stages generate 335 ± 5 μJ of signal energy with 110 ± 5 pJ fluorescence averaged over 500 shots at 10 Hz repetition rate. The pump and seed pulse energies both have root mean square stabilities (RMS) of 1%.

From these measurements, the energy contrast, shown in Fig. 7b, between the OPA signal and fluorescence improves considerably by a factor of ~ 500 from 6×10^3 to 3×10^6 with greater pump depletion, producing a maximum total gain of 2.7×10^5 for the primary laser seed. Increasing the seed energy E_s (i.e. greater pump depletion) has been found to follow a convenient $\propto E_s^{1/\sqrt{2}}$ relationship in the observed energy contrast.

Due to the 20 nm finite bandwidth acceptance of the stretcher and the compressor in the beamline following the ps-OPAs, only 12% of the broadband fluorescence, as shown in Fig. 4, will propagate through the system. Therefore, the parametric fluorescence from the ps-OPAs is estimated to contribute a temporal intensity contrast of 3×10^{-9} at 1.3 ps before the peak of the primary laser pulse after compression, using identical modelling to that shown in Fig. 3. Pump depletion can therefore be seen as a highly desirable characteristic in an OPA to maximise the temporal contrast with respect to parametric fluorescence. This experimental analysis agrees with numerical modelling of fluorescence in pump depletion by Manzoni et al. [14].

3.1. Parametric fluorescence input noise

The semi-classical origin of parametric fluorescence is generally accepted to be the zero-point fluctuations of the electromagnetic field acting as a seed source for OPA in the non-linear crystal. The absolute number of background seed photons can be estimated using the small-signal gain values of the OPA stages in the undepleted pump regime. This gain value can be extracted from the experimental data in Fig. 7a, where the undepleted pump regime exists for very low laser seed energies, and is found to be $1.3 \pm 0.2 \times 10^8$ for the Gaussian temporal and spatial profiles of the pulses. It should be noted that this value fits well with an analytical value of 2.12×10^8 for the small signal gain using a plane-wave approximation.

In the undepleted regime, 6.2 ± 0.5 nJ of fluorescence is observed directly downstream from the OPA, meaning that 300 ± 25 seed photons, or 0.7 ± 0.1 photons $\mathrm{ps}^{-1}\,\mathrm{nm}^{-1}$ were needed to produce this amount of fluorescence in the OPA process at these wavelengths.

The absolute level of spontaneous fluorescence seed in an OPA amplifying a 532 nm CW laser in BBO was determined experimentally by Homann and Riedle to be 7.7 photons $\mathrm{ps}^{-1}\,\mathrm{nm}^{-1}$ [15]. This agreed within a factor of 1.4 to a formula adapted from

stimulated Raman scattering theory to determine the effective number of noise seed photons N_{eff} in its parametric fluorescence analogue in OPA [15]:

$$N_{eff} = \frac{n^3 \Delta\lambda c \tau}{\pi \lambda^2} \quad (1)$$

where n is the refractive index of the signal in the non-linear amplifier medium, λ and $\Delta\lambda$ are the central wavelength and the observable bandwidth of fluorescence produced respectively, c is the speed of light and τ is the fluorescence pulse duration. It should be noted that this equation matches very closely with those reported in [1,8]. When applied our ps-OPA observations of 200 nm bandwidth centred at 1020 nm with 6 ps pump pulses, Eq. (1) yields a value of 170 photons, or 0.4 photons ps^{-1} nm^{-1}, which agrees within a factor of 1.75 to the experimental determination of the seed source for our ps-OPA stages. Possible discrepancy between the two values may be due to measurement error of the small signal gain, as the 0.3 pJ seed in the undepleted regime is more prone to systematic error of the photodiode calibration with a very weak signal.

3.2. Fluorescence statistics

The fluorescence energies reported above have so far only considered average values measured over >500 shots. The shot-to-shot variation of fluorescence from the OPA stages, shown in Fig. 8, has been observed to fluctuate significantly, with ~63% RMS deviation, compared to the 1% RMS deviation of the OPA pump and laser seed pulses. This indicates that the large fluorescence fluctuations observed are an unavoidable consequence of the exponential photon distribution of the vacuum fluctuations [16]. The observed Poisson-like distribution of the fluorescence energy supports the case for a randomly fluctuating seed term.

The significance of these large fluctuations on experiments sensitive to the temporal contrast is the relatively small shot-to-shot probability of the fluorescence contribution to the temporal contrast increasing to an unacceptably high level. For our ps-OPA system, there is a 1.5% probability of fluorescence becoming 5 times greater than the mean and a 0.3% chance for a ten-fold increase in fluorescence on a single shot.

4. Conclusions

We have demonstrated a simple and effective method to directly characterise the parametric fluorescence emission from a seeded picosecond-regime OPA system operating at high gain without requiring additional amplifiers or a chirped-pulse compressor to resolve the weak fluorescence signal. This method can in principle be applied to any OPA system that generates fluorescence bandwidth that is not contained in the seed and can be spectrally filtered to clearly discriminate it from the amplified seed light.

We have determined that the seeded OPA fluorescence emission intensity is directly linked to the pump intensity in the non-linear crystal and that depletion of the available pump energy from amplification of the primary laser seed greatly reduces the fluorescence generated. We observed that the fluorescence energy decreases by a factor of ~60 when achieving pump-depletion for pump pulses five times longer in duration than the seed, yielding a contrast enhancement factor of ~500 from undepleted to maximum pump depletion at the intensity maxima. It is expected that the fluorescence can be reduced by increasing the seed duration to further increase pump depletion in the temporal wings of the pump pulse, improving energy extraction at the cost of bandwidth amplification.

The determination of the laser seeded OPA absolute fluorescence energy, bandwidth and pulse duration was sufficient to determine the contrast limitation it imposes after compression. When applied to our ps-OPA system, we have estimated the fluorescence emission from these OPAs after compression that will contribute a 2.1 ps pedestal with 3×10^{-9} temporal intensity contrast 1.3 ps before the peak of the primary laser pulse. In addition to pump-depletion in the OPAs, blocking the broadband fluorescence bandwidth outside of the laser bandwidth in the downstream pulse stretcher and compressor further reduced the fluorescence intensity and improves the intensity contrast on target.

The mean absolute level of the incoherent fluorescence seed source has been experimentally determined to be 0.7 ± 0.1 photons ps^{-1} nm^{-1}. The random intensity fluctuations of the fluorescence seed will contribute to a population of 1.5% of shots with five times greater fluorescence intensity and 0.3% probability of a ten-fold increase in the mean fluorescence intensity.

Knowledge of this noise source term, its mechanism of amplification and intensity fluctuation statistics in a seeded OPA process will be beneficial in the modelling and assessment of the potential impact of parametric fluorescence pre-pulse in high-intensity laser–matter interaction experiments.

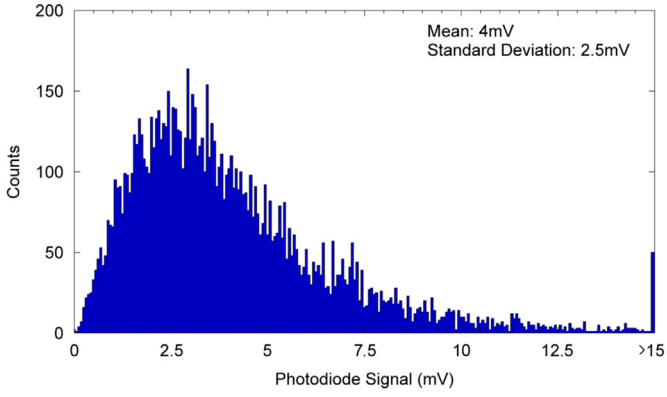

Fig. 8. Measured photon statistics of the parametric fluorescence producing a Poisson distribution, demonstrating the random nature of the fluorescence seed, which can occasionally produce much brighter fluorescence background from shot-to-shot as a result.

Acknowledgements

We gratefully acknowledge funding from EPSRC grant EP/G001324/1 and an AWE Industrial CASE Studentship. We are pleased to recognise useful discussions with N. Hopps, P. Treadwell and D. Hillier of the AWE Orion Laser Facility and the technical assistance provided by Melvin Patmore and Brian Willey.

References

[1] I.N. Ross, P. Matousek, M. Towrie, A.J. Langley, J.L. Collier, Opt. Commun. 144 (1–3) (1997) 125. http://dx.doi.org/10.1016/S0030-4018(97)00399-4.
[2] R. Glauber, F. Haake, Phys. Lett. A 68 (1) (1978) 29. http://dx.doi.org/10.1016/0375-9601(78)90747-8.
[3] D. Hillier, C. Danson, S. Duffield, D. Egan, S. Elsmere, M. Girling, E. Harvey, N. Hopps, M. Norman, S. Parker, P. Treadwell, D. Winter, T. Bett, Appl. Opt. 52 (18) (2013) 4258. http://dx.doi.org/10.1364/AO.52.004258, WOS:000320708500022.
[4] E.W. Gaul, M. Martinez, J. Blakeney, A. Jochmann, M. Ringuette, D. Hammond, T. Borger, R. Escamilla, S. Douglas, W. Henderson, G. Dyer, A. Erlandson, R. Cross, J. Caird, C. Ebbers, T. Ditmire, Appl. Opt. 49 (9) (2010) 1676. http://dx.doi.org/10.1364/AO.49.001676.
[5] C. Dorrer, I.A. Begishev, A.V. Okishev, J.D. Zuegel, Opt. Lett. 32 (15) (2007) 2143. http://dx.doi.org/10.1364/OL.32.002143, WOS:000249087200025.
[6] F. Tavella, K. Schmid, N. Ishii, A. Marcinkevicius, L. Veisz, F. Krausz, Appl. Phys. B 81 (6) (2005) 753. http://dx.doi.org/10.1007/s00340-005-1966-3.

[7] I.N. Ross, G.H.C. New, P.K. Bates, Opt. Commun. 273 (2) (2007) 510. http://dx.doi.org/10.1016/j.optcom.2007.01.033, WOS:000245847800034.
[8] I. Musgrave, W. Shaikh, M. Galimberti, A. Boyle, C. Hernandez-Gomez, K. Lancaster, R. Heathcote, Appl. Opt. 49 (33) (2010) 6558. http://dx.doi.org/10.1364/AO.49.006558.
[9] S. Luan, M. Hutchinson, R. Smith, F. Zhou, Meas. Sci. Technol. 4 (12) (1993) 1426. http://dx.doi.org/10.1088/0957-0233/4/12/018.
[10] F. Tavella, A. Marcinkevicius, F. Krausz, New J. Phys. 8 (2006) 219. http://dx.doi.org/10.1088/1367-2630/8/10/219, WOS:000241207200001.
[11] X.-L. Li, H.-J. Liu, H.-Y. Wang, W. Zhao, S.-X. Shi, J. Mod. Opt. 55 (11) (2008) 1795. http://dx.doi.org/10.1080/09500340701813202.
[12] D. Bigourd, S. Patankar, S.I.O. Robbie, H.W. Doyle, K. Mecseki, N. Stuart, K. Hadjicosti, N. Leblanc, G.H.C. New, R.A. Smith, Appl. Phys. B 113 (4) (2013) 627. http://dx.doi.org/10.1007/s00340-013-5519-x.
[13] D.A. Kleinman, Phys. Rev. 174 (3) (1968) 1027. http://dx.doi.org/10.1103/PhysRev.174.1027.
[14] C. Manzoni, J. Moses, F.X. Kärtner, G. Cerullo, Opt. Express 19 (9) (2011) 8357. http://dx.doi.org/10.1364/OE.19.008357.
[15] C. Homann, E. Riedle, Laser Photon. Rev. 7 (4) (2013) 580. http://dx.doi.org/10.1002/lpor.201200119 (WOS:000325934600019).
[16] J.P. Gordon, W.H. Louisell, L.R. Walker, Phys. Rev. 129 (1) (1963) 481. http://dx.doi.org/10.1103/PhysRev.129.481.